Astron. Astrophys. 322, 419–426 (1997)

ASTRONOMY
AND
ASTROPHYSICS

Molecular excitation in Centaurus A: the ^{13}CO J=1–0 map and CO line ratios⋆

W. Wild[1,2], **A. Eckart**[3], **and T. Wiklind**[4]

[1] IRAM, Avda. Divina Pastora 7, E-18012 Granada, Spain
[2] European Southern Observatory, Casilla 19001, Santiago 19, Chile
[3] Max-Planck-Institut für extraterrestrische Physik, D-85740 Garching bei München, Germany
[4] Onsala Space Observatory, S-43900 Onsala, Sweden

Received 27 September 1996 / Accepted 3 December 1996

Abstract. We present a fully sampled map of the ^{13}CO J=1–0 emission in the dust lane of Centaurus A as well as ^{13}CO 2–1 and for the first time C^{18}O 1–0 spectra at selected positions. The morphology of the ^{13}CO map is similar to the ^{12}CO 1–0 and 2–1 maps. Maps of the ^{12}CO 2–1/1–0 and ^{12}CO/^{13}CO 1–0 ratios show small variations of the ratios throughout the disk with a rise of the ^{12}CO 2–1/1–0 ratio towards the southeast. The values found are within the range as found in other galaxies. Radiative transfer calculations indicate a kinetic temperature of 10–15 K and H_2 densities on the order of 3×10^4 cm^{-3}. In the southeastern part of the dust lane, the gas appears to be warmer (20–30 K) which may be due to a greater star formation activity. The total molecular mass is about 1.2×10^8 M$_\odot$.

The observed ^{12}CO 2–1 intensity is consistent with the molecular gas being distributed in a thin, warped disk as modelled by Quillen et al. (1992). Comparison of the measurements with the kinematic model shows good agreement.

Key words: galaxies: individual: NGC 5128 – galaxies: nuclei – galaxies: ISM – radio lines: galaxies

1. Introduction

Centaurus A (NGC 5128) is the closest radio galaxy. At a distance of only about 3 Mpc (de Vaucouleurs 1979) we are able to study the properties of this peculiar elliptical galaxy with its prominent dust lane in great detail and at high spatial resolution ($1'' \widehat{=} 15$ pc).

Optical observations show that the dust lane is warped and contains a ring of H II regions (Dufour et al. 1979, Graham 1979, Bland et al. 1987). Investigations of the neutral interstellar medium in Centaurus A using the 21cm H I emission have been carried out by van Gorkom (1987) and van Gorkom et al. (1990). The molecular interstellar medium in the dust lane has been studied by a number of authors (e.g. Phillips et al. 1987, Eckart et al. 1990a, 1990b, Israel et al. 1990, 1991, Quillen et al. 1992, Rydbeck et al. 1993). The 158μm [CII] fine structure line at the nucleus has been measured by Crawford et al. (1985) and Madden et al. (1992). The far-IR continuum emission has been observed with IRAS (DSD data: Marston and Dickson 1988 and CPC IRAS data: Eckart et al. 1990a) and from the KAO (Joy et al. 1988).

The combination of the optical, far-infrared, and radio spectroscopic investigations has demonstrated intense star formation within the dust lane of this elliptical radio galaxy. In this context it is of special interest to study the properties of the molecular gas reservoir out of which the star formation process is fed.

This is the fourth in a series of papers about the molecular interstellar medium of Centaurus A. In three previous papers we presented a fully sampled map of the ^{12}CO J=1–0 emission together with *IRAS* observations of the far-IR continuum (Eckart et al. 1990a, Paper I), measurements of the millimeter absorption lines towards the nucleus (Eckart et al. 1990b, Paper II), and a ^{12}CO J=2–1 map along the dust lane at a resolution of 22″ (Rydbeck et al. 1993, Paper III). Using deconvolution techniques a molecular circumnuclear ring of radius ∼100 pc was inferred. While in Paper III we studied the kinematics of the nuclear molecular gas only, here we will use the CO J=2–1 data in combination with new isotopic CO data to investigate the excitation conditions and the kinematics throughout the disk.

In this paper we present the first fully sampled ^{13}CO J=1–0 map along the dust lane of Centaurus A, as well as spectra of the ^{13}CO J=2–1 emission in the disk and C^{18}O J=1–0 emission at two positions. These new data allow us, in combination with the ^{12}CO J=1–0 and J=2–1 maps which we presented earlier (Papers I and III), to study the column density, number density, and excitation temperature of the molecular gas in detail throughout the dust lane. In addition we compare the ^{12}CO J=2–1 map structure with the kinematic model of the gas disk by Quillen et al. (1992).

Send offprint requests to: W. Wild, wild@iram.es

⋆ Based on observations collected at the European Southern Observatory, La Silla, Chile

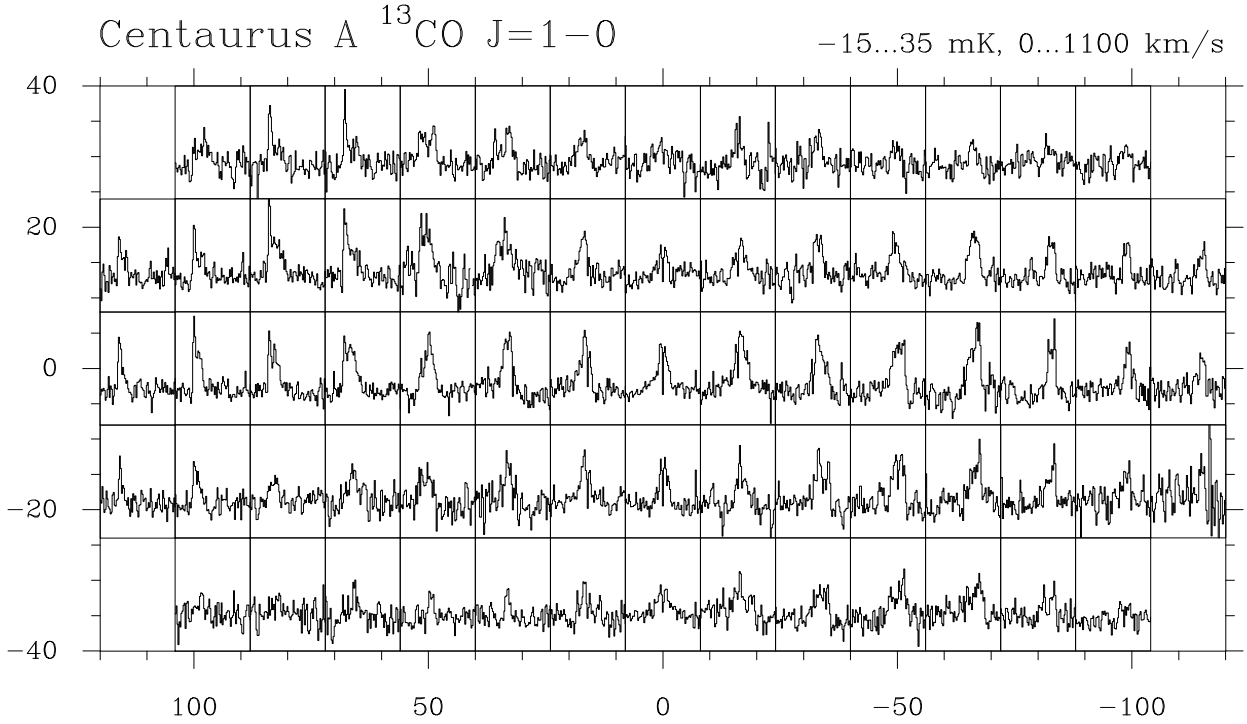

Fig. 1. ^{13}CO J=1–0 spectra along the dust lane of Centaurus A taken at a spacing of 16″ on a grid rotated by a position angle of 125°. In each spectrum the velocity axis ranges from 0 to 1100 km s^{-1} and the antenna temperature (T_A^*) axis from –15 to +35 mK. The (0,0) position corresponds to $\alpha(1950) = 13^h22^m31.8^s$, $\delta(1950) = -42°45'30''$. Offsets are parallel and perpendicular to the dust lane, respectively, and in units of arc seconds.

2. Observations

All observations were carried out with the 15m Swedish-ESO Submillimetre Telescope (SEST) on La Silla, Chile. The adopted central position for Centaurus A was $\alpha(1950) = 13^h22^m31.8^s$, $\delta(1950) = -42°45'30''$. The FWHM beam widths of SEST are 44″ at 110.201 GHz (^{13}CO 1–0), 45″ at 109.782 GHz (C^{18}O 1–0), and 22″ at 220.399 GHz (^{13}CO 2–1). Main beam efficiencies are $\eta_{110GHz} = 0.68$ and $\eta_{220GHz} = 0.6$.

We observed in the dual beam switching mode, *i.e.* a chopper wheel switched between two positions on the sky displaced by about 12′ in azimuth. First the source was placed in one beam and then in the other beam. The backend was the low resolution acousto-optical spectrometer with a used bandwidth of 500 MHz (≙1360 km/s at 110 GHz, 680 km/s at 220 GHz) and 720 channels. The system was calibrated with the chopper wheel method. Pointing was checked frequently using the nuclear continuum source of Centaurus A and the nearby (distance ∼ 17°) SiO maser W Hya and is estimated to be accurate to within 3″.

We mapped the ^{13}CO J=1–0 emission in an area of about 220″×65″ around the dust lane in several observing runs between January 1992 and March 1993 using a dual polarization 3 mm Schottky receiver. The system temperature during the observations ranged from 350 K to 650 K. A total of 71 positions was observed on a grid with a spacing of 16″ and a position angle of 125° . The spectra are shown in Fig. 1. Each position was observed several times (typically 2 to 4 times) on different observing runs. The total integration time per position for almost all of the positions was 128 min with the exception of a few positions which were observed with integration times ranging from 64 min to 224 min.

The ^{13}CO J=2–1 spectrum at offset ($\Delta\alpha$, $\Delta\delta$) =(–52″, 37″), Fig. 2, was obtained with a single polarization 1.3 mm SIS receiver in May 1993. The system temperature was about 900 K and the integration time 712 min.

The C^{18}O J=1–0 spectrum at the central position (Fig. 4) with the ^{13}CO J=1–0 line in the same band was obtained in January 1994 with the 3 mm Schottky receiver. The system temperature was around 440 K and the integration time 648 min. The C^{18}O J=1–0 emission in the disk (Fig. 3) was measured in January 1996 with a 3 mm SIS receiver. The system temperature was around 220 K and the integration time 912 min.

3. Results and discussion

3.1. The ^{13}CO J=1–0 map

A map of the velocity integrated ^{13}CO J=1–0 emission along the dust lane is shown in Fig. 5 (upper panel) together with the ^{12}CO 2–1 and 1–0 maps. The emission is well concentrated along the dust lane. The overall spatial variation is quite similar to the ^{12}CO J=1–0 and J=2–1 maps.

All three CO maps show two peaks of emission separated by about 90″ (∼650 pc radius) and symmetrically displaced

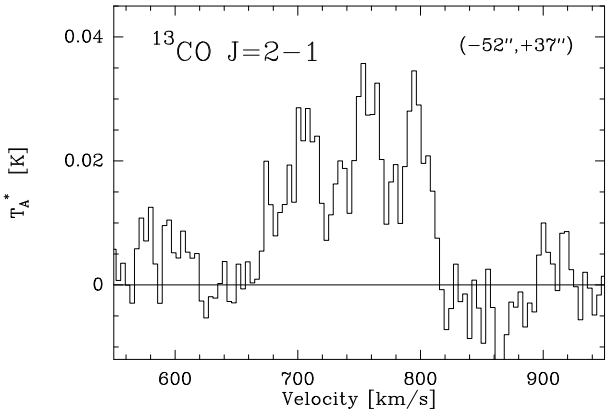

Fig. 2. ^{13}CO J=2–1 spectrum in the disk of Centaurus A at offset position ($\Delta\alpha, \Delta\delta$) =(–52″, 37″).

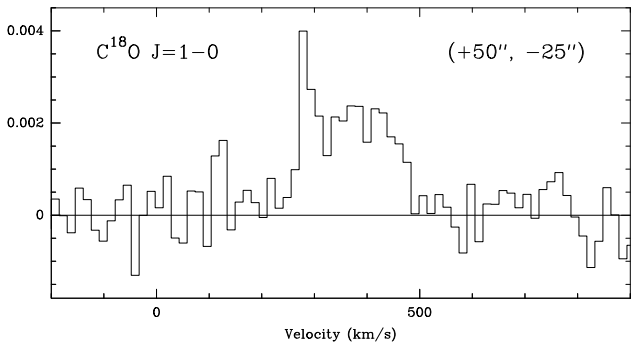

Fig. 3. C^{18}O J=1–0 spectrum at offset position ($\Delta\alpha, \Delta\delta$) =(+50″, –25″) in the southeastern part of the disk. The vertical axis shows antenna temperature.

from the central position. A slight warp along the dust lane (more clearly visible in the ^{12}CO J=2–1 and J=1–0 maps than in the ^{13}CO 1–0 map) is present in all three maps. This warp is very pronounced in both deconvolved ^{12}CO 2–1 maps (see Paper III, Fig. 1). The good agreement of the ^{12}CO and ^{13}CO emission suggests that the two CO isotopes are probing the same molecular gas.

3.2. ^{13}CO J=2–1 spectrum

Fig. 2 shows the ^{13}CO J=2–1 spectrum at offset ($\Delta\alpha, \Delta\delta$) = (–52″, +37″) in the disk. This position is close to one of the maxima of the ^{13}CO J=1–0 map. The velocity width is about 130 km/s, identical to the width seen in the ^{12}CO 2–1 spectrum, and less than the width of the ^{13}CO 1–0 spectrum due to the difference in beam size. The ^{13}CO 2–1 spectrum shows more structure as compared to ^{12}CO 2–1 which may indicate varying optical depth of ^{13}CO with velocity.

Due to the weakness of the emission only one ^{13}CO J=2–1 spectrum in the disk could be obtained within the constraints of observing time. However, together with the ^{13}CO 2–1 measurement at the central position (Paper I) and using the ^{12}CO 2–1, ^{12}CO 1–0 and ^{13}CO 1–0 maps, we can investigate possible differences in excitation between the center and the disk.

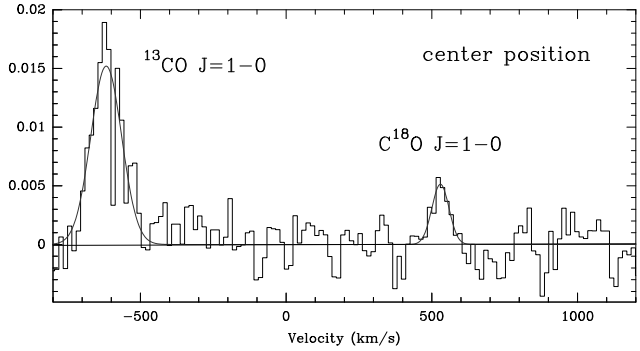

Fig. 4. C^{18}O J=1–0 spectrum at the center of Centaurus A with the ^{13}CO J=1–0 line appearing in the same band. The central absorption feature is clearly visible in ^{13}CO. The velocity axis is with respect to the C^{18}O line. The vertical axis shows antenna temperature.

3.3. C^{18}O J=1-0 spectra

For the first time we obtained spectra in the C^{18}O J=1–0 transition in the disk (Fig. 3) at the southeastern offset position ($\Delta\alpha, \Delta\delta$) =(+50″, –25″) and on the nucleus (Fig. 4). The spectrum at the nuclear position was obtained together with the ^{13}CO J=1-0 line measured in the same band. The similar width and line shapes of both lines demonstrate that the same molecular gas is probed and that the line ratios can be used in radiative transfer programs to determine the beam averaged properties of the molecular gas in the disk of Centaurus A. This simultaneous measurement allows a very well calibrated determination of the ^{13}CO(1-0)/C^{18}O(1-0) line ratio. This ratio is 5 and convincingly shows, in comparison to the expected isotopic line ratio of 8, that the overall optical depth in the two isotopic lines must be low.

The C^{18}O J=1–0 spectrum in the disk has the same line width and shape as the ^{12}CO 1–0 spectrum at this position, again indicating that the two isotopic lines sample the same gas.

3.4. The central absorption feature and C^{18}O J=1–0

The combination of a radio source (which is strong at millimeter wavelengths) and a large column density of obscuring gas (the extinction towards the nucleus of Cen A is estimated to be more than 15 mags, Paper I), gives rise to a number of molecular absorption lines along the line of sight towards the center of Cen A (cf. Paper II, Seaquist & Bell 1990, Israel et al. 1990, 1991). The molecular absorption probes a region with an extent limited by the size of the radio core. VLBI observations give a size of the core of $<$0.5 milliarcsec (Preston et al. 1983), corresponding to $< 7.3 \times 10^{-3}$ pc if Cen A is at a distance of 3 Mpc.

The opacity of a molecular rotational absorption line is proportional to T_x^{-2} (with T_x being the excitation temperature), which makes absorption lines most sensitive to excitationally cold gas, i.e. diffuse gas. For instance, if equal column densities

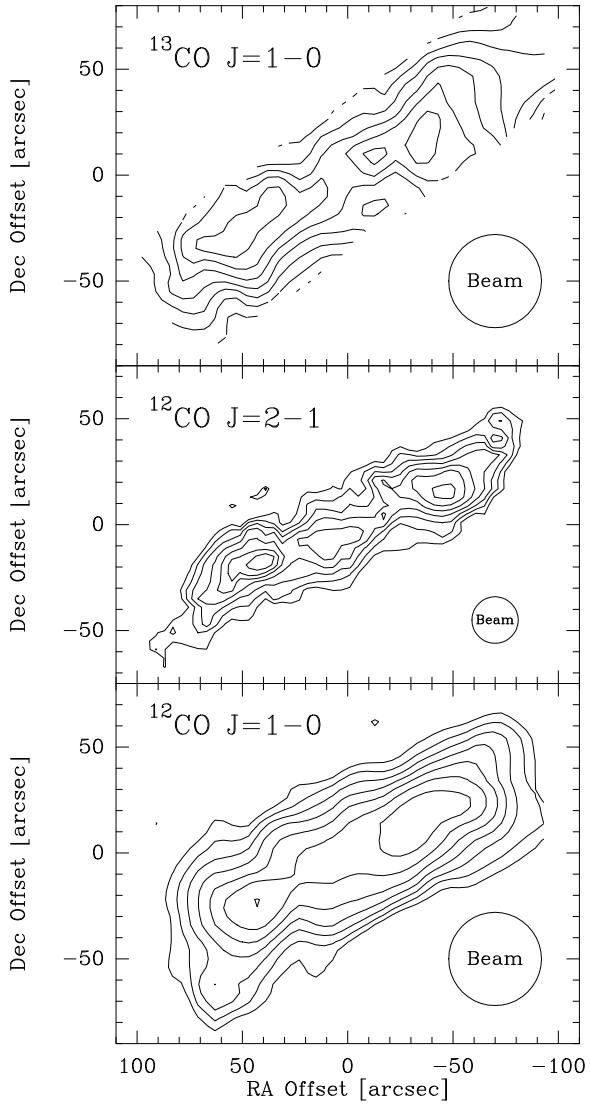

Fig. 5. Contour maps of Centaurus A in different CO lines. *Upper panel:* the velocity integrated ^{13}CO J=1–0 emission along the dust lane. The contour intervals are 0.5, 1.0, 1.5, ... K km s^{-1}. *Middle panel:* Contour map of the integrated ^{12}CO J=2–1 emission. Contours are 20, 25, 30, ... K km s^{-1}. *Lower panel:* Map of the integrated ^{12}CO J=1–0 emission (from Paper I). The morphological appearance is quite similar for the three maps.

of warm (20 K) and cold (5 K) gas exist along a line of sight, the cold component will contribute more than 90% of the opacity to the CO(1–0) line seen in absorption, whereas the warm gas component will dominate the emission.

The ^{13}CO(1–0) line shows a distinct absorption line close to the systemic velocity of Cen A. Our C^{18}O(1–0) spectra (Fig. 4) only gives an upper limit to any absorption line. We can, however, use this to derive a lower limit to the N(^{13}CO)/N(C^{18}O) ratio. This limit can then be used to compare the dense and warm gas, giving rise to the emission, with the diffuse gas component.

The non-detection of the C^{18}O absorption feature allows to derive an upper limit of the C^{18}O J=1–0 optical depth. For the absorption line depth $T_{\rm abs}$ one finds (see Paper II):

$$T_{\rm abs} \approx -T_{\rm con}(1 - e^{-\tau}). \quad (1)$$

where $T_{\rm con}$ is the beam diluted continuum background (= 0.29 K at 110 GHz) and τ the optical depth. We can give a limit of 5 mK on the absorption feature in the (unsmoothed) central C^{18}O J=1-0 spectrum at the systemic velocity of Centaurus A. This yields an upper limit for the opacity of the C^{18}O line

$$\tau_{18} \approx -\ln\left[1 + \frac{T_{\rm abs}}{T_{\rm con}}\right] < 0.018 \quad (2)$$

Another way to estimate the optical depth τ_{18} in the C^{18}O(1-0) line makes use of the simultaneous measurement of the central ^{13}CO and C^{18}O J=1–0 emission within the same band. To obtain the optical depth τ_{18} we can calculate the ratio of the ^{13}CO(1-0) and the limit of the C^{18}O(1-0) absorption. Assuming that the ^{13}CO(1-0) and C^{18}O(1-0) absorption lines have similar width and using the ratio of measured ^{13}CO integrated absorption line I_{13} = 0.44 K km s^{-1} and the upper limit $I_{18} < 0.02$ K km s^{-1} for C^{18}O, we obtain

$$\frac{-T_{\rm con}(1 - e^{-\tau_{13}})}{-T_{\rm con}(1 - e^{-\tau_{18}})} \approx \frac{I_{13}}{I_{18}} = \frac{0.44}{< 0.02} > 22 \quad (3)$$

Using the ^{13}CO(1-0) optical depth of τ_{13}=0.7 derived in Paper II we get an upper limit on the C^{18}0(1-0) optical depth of $\tau_{18}<0.02$ which is consistent with the value derived above.

Adopting the same line width for the ^{13}CO(1–0) and the (non-detected) C^{18}O(1–0) absorption lines, the optical depths given above give a column density ratio N(^{13}CO)/N(C^{18}O) > 30. We have used an excitation temperature of 5 K, but the abundance ratio is more or less independent of the adopted $T_{\rm x}$.

Whereas the ^{12}CO/^{13}CO and ^{13}CO/C^{18}O ratios derived from the emission profiles in Cen A indicate that the properties of the molecular gas are similar to those found for the disk material in other galaxies, the N(^{13}CO)/N(C^{18}O) ratio derived from the absorption data shows that the diffuse gas is different. It seems that the diffuse gas, causing the absorption, is deficient in C^{18}O.

The isotope ^{18}O is believed to be produced in massive stars, whereas ^{13}C is produced in intermediate mass stars. ^{13}C is in fact fully converted into ^{14}N in massive stars (cf. Wilson & Matteuchi 1992). The low abundance of C^{18}O in the diffuse gas of Cen A is therefore consistent with massive star formation taking place in the denser and warmer gas seen in emission and not in the diffuse gas – a situation which is similar to the star formation in our Galaxy.

3.5. Molecular emission line ratios

The ratios of molecular line intensities are powerful diagnostic tools for the investigation of the molecular ISM. Since the intensities of different CO transitions depend on H_2 number density, temperature and optical depth of the molecular gas, one can draw conclusions on the physical parameters using the intensity

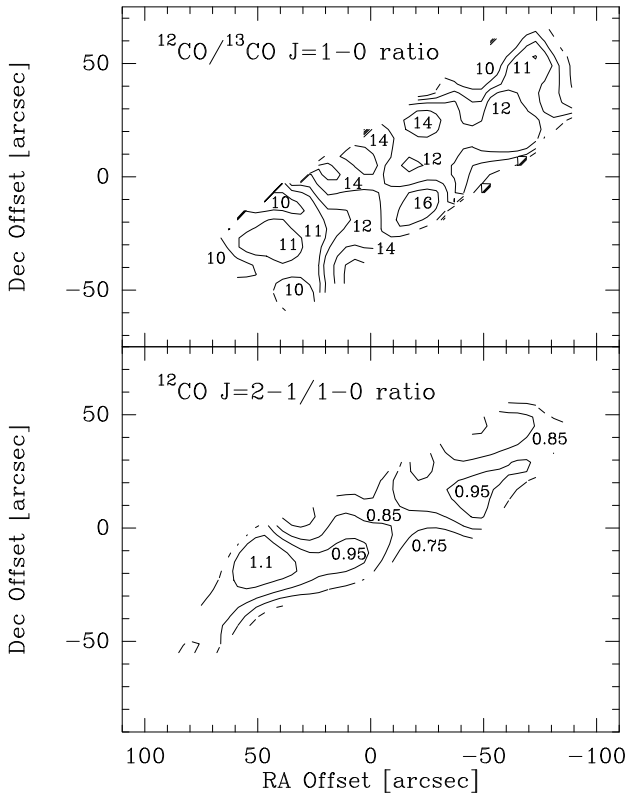

Fig. 6. *Upper panel:* Map of the isotopic ^{12}CO/^{13}CO J=1–0 ratio. *Lower panel:* Map of the ^{12}CO J=2–1/1–0 ratio along the disk of Centaurus A. Contours are 0.75, 0.85, 0.95, and 1.1 . The ratio rises towards the southeastern part of the disk. The 2–1 map has been convolved to the 1–0 resolution before calculating the ratio.

ratios. It is particularly important to take into account the measurements of optically thinner isotopic ^{13}CO and C^{18}O lines in order to sample deeper into the molecular gas. Unfortunately, this proves difficult – or even impossible – for many galaxies because of their weak isotopic CO emission. Centaurus A is one of the few galaxies where these measurements can be carried out.

Maps of the isotopic ^{12}CO/^{13}CO J=1–0 ratio and the velocity integrated intensity ratio of ^{12}CO J=2–1/1–0 are shown in Fig. 6. Before calculating the ^{12}CO J=2–1/1–0 ratio, the J=2–1 map was convolved with a Gaussian beam to the resolution of the J=1–0 data (44″). We have restricted the 2–1/1–0 ratio map to the spatial extent of the original (unconvolved) 2–1 map.

In Centaurus A the isotopic ^{12}CO/^{13}CO ratio is highest (14–16) close to the central position, and falls off along the dust lane. The overall ratio of 10 to 16 is well within the range as found in other external galaxies (*e.g.* Young and Sanders 1986, Sage and Isbell 1991). The ^{12}CO J=2–1/1–0 line ratio lies in the range 0.75 to 0.95 in the largest part of the disk, except in the SE where it rises to 1.1 . For the 2–1 and 1–0 lines of the same isotope one expects a 2–1/1–0 ratio of about 0.9 for moderately warm ($T_{\rm kin} \geq 15$ K), optically thick gas, and 4 for dense, warm and optically thin gas. A ratio of less than 0.9 can arise in the case of colder or subthermally excited gas. More quantitative results are obtained by radiative transfer calculations (see following section). For the central position, our ratio agrees well with the value of Paper I. However, for positions in the disk, the ratios are up to a factor of two higher than previously determined in Paper I on the basis of the ^{12}CO J=2–1 spectra of Phillips et al. (1987) which were the only data available for this transition at that time. The ratios presented here are much more reliable since we measured each ^{12}CO J=2–1 spectrum on several occasions. Regular checks of the long term calibration stability at SEST show a maximum variation of ±10% (L. Nyman, priv. comm.).

Table 1. CO emission line ratios at the center and the disk of Centaurus A.

Line ratio	center	disk at offset (–52″, +37″)	disk at offset (+50″, –25″)
^{12}CO 2–1/1–0	0.85 ± 0.1	0.85 ± 0.1	1.1 ± 0.1
^{13}CO 2–1/1–0	1.0 ± 0.2	0.85 ± 0.2	
^{12}CO/^{13}CO 1–0	14 ± 3	11 ± 2	11 ± 2
^{12}CO/C^{18}O 1–0	75 ± 25		85 ± 25

Table 1 lists the CO emission line ratios determined at the center and two positions in the disk of Centaurus A. The source size correction for calculating the ^{13}CO 2–1/1–0 ratio was carried out assuming that the CO emission has a Gaussian full half-width of 30″ perpendicular and is much larger than the beam parallel to the dust lane. The ^{12}CO/C^{18}O ratio of 75 at the central position is in agreement with the value of > 55 given in Paper I.

3.6. Radiative transfer models and H_2 mass estimate

In order to obtain more quantitative results on the molecular excitation in the simple "one component" case we calculated radiative transfer models. These models take non-LTE effects, clumping, and optical depth dependent filling factors into account, and assume that the emission of ^{12}CO, ^{13}CO , and C^{18}O all arise in regions with similar physical conditions. While such simple one component models certainly underestimate the complex structure of the molecular interstellar medium on a small scale, they are still useful for the investigation of the large scale, average properties of the molecular gas. In particular, differences in excitation and column densities across the disk of Centaurus A should manifest themselves in the molecular line ratios.

The model calculations consist of two steps. First, we compute the populations of the 10 lowest rotational levels of ^{12}CO and ^{13}CO as a function of kinetic temperature, molecular hydrogen density, and CO column density. We assumed statistical equilibrium and fractional abundances as they are commonly found and quoted for dense molecular clouds in the Galaxy (Millar and Freeman 1984, Graedel, Langer and Frerking 1982, Wannier 1980): [^{12}CO]/[H_2]=8×10^{-5}, [^{12}CO]/[^{13}CO]=60, and [^{12}CO]/[C^{18}O]=500. Second, we assumed a clumpy cloud

Table 2. Derived physical parameters for the center and disk of Centaurus A.

Offset position	$T_{\rm kin}$ [K]	$n(H_2)$ [cm^{-3}]	N(CO) [cm^{-2}]
center	10 – 15	3×10^4	$3 - 4 \times 10^{17}$
(–52″, +37″)	10 – 15	$1 - 3 \times 10^4$	$3 - 4 \times 10^{17}$
(+50″, –25″)	20 – 30	$1 - 3 \times 10^4$	1×10^{18}

model following Martin, Sanders and Hills (1984). A more detailed description of the model is given in Eckart et al. (1990c).

Kinetic temperature, number density, and column density of the molecular gas are constrained by both the line ratios given in Table 1 and the comparison of predicted to measured line intensity.

Table 2 summarizes the results from the model calculations. The "best physical parameters" for the center position and the disk offset position ($\Delta\alpha, \Delta\delta$) =(–52″, +37″) can be described as follows: The beam averaged CO column density is of the order of $3 - 4 \times 10^{17}$ cm^{-2}, the molecular hydrogen volume density $n(H_2) \approx 3 \times 10^4$ cm^{-3}, and the kinetic gas temperature 10 – 15 K. Throughout the disk the model calculations indicate high optical depths for the ^{12}CO J=1–0 ($\tau_{10} \sim 5 \ldots 10$) and J=2–1 ($\tau_{21} \sim 10 \ldots 20$) line.

At offset position (+50″, –25″) the gas appears to be warmer (20–30 K), and the beam averaged CO column density somewhat higher ($\sim 1 \times 10^{18}$ cm^{-2}). This result is mainly due to the higher CO 2–1/1–0 ratio measured at this position. The KAO far-IR data of Joy et al. (1988) show a secondary peak $\sim$60″ to the southeast which coincides with the region of the higher ^{12}CO ratio. Stronger H I, Hα and [N II] emission are also seen in the southeastern part of the dust lane (van Gorkom et al. 1990, Bland et al. 1987, Nicholson et al. 1992). In Paper I we argued that a possible explanation is a stronger UV-field giving rise to a larger fraction of the ISM being in photodissociated regions and a smaller relative amount of H_2. With the additional information of the ^{13}CO and C^{18}O spectra and more line ratios, the radiative transfer calculations indicate not only on average warmer molecular gas in the SE, but also a higher CO column density leading to a larger H_2 content (for constant relative [CO]/[H_2] abundances). A greater star-formation activity in the SE (as already speculated in Paper I) could explain the warmer molecular gas and stronger Hα and [N II] emission. Further support for this explanation comes from the fact that the 158μm [C II] emission extends more into the southeastern part of the disk than into the northwestern part (R. Genzel, unpublished map).

With an average ^{12}CO column density of 5×10^{17} cm^{-2} across the disk (taking into account the ^{12}CO column density of 3×10^{17} cm^{-2} in large parts of the disk and the higher value of 1×10^{18} cm^{-2} in the southeast, as obtained from our model calculations) we derive a H_2 mass of 1.2×10^8 M$_\odot$. This is somewhat lower than the H_2 estimate of 1.8×10^8 M$_\odot$ based on model calculations for the central position alone (Paper I).

3.7. Kinematics of the molecular gas

Our data also allow a detailed comparison of the measured map structure with the kinematic model of the gas disk in Centaurus A as given by Quillen et al. (1992). This comparison is best done using the ^{12}CO 2–1 data because of the higher spatial resolution. Quillen et al. (1992) explain the velocity field observed towards the dust lane of Centaurus A in terms of a differentially precessing gas disk. In their model the inclination of the major axis potential is 60°$\pm$7° with the gas at an angle of 25°$\pm$5° above the equatorial plane of the potential. The velocity of the gas is 290 km/s $\pm$ 20 km/s. This indicates that in beams with widths of the order of half an arcminute the expected velocity broadening of the line just due to this peculiar geometry is about 130 km/s. In addition there is a beam width dependent contribution from the overall gradient of the rotation curve of 3.1 km/s per arcsecond.

For the ^{12}CO(2–1) line in a 22″ beam we measure a mean line width in the velocity position diagram of 150 km/s $\pm$ 10 km/s. For the ^{12}CO(1–0) line with a resolution of 45″ we find a mean line width of 210 km/s (Paper I). Correcting for the contribution of the straight rotation curve and the finite beam width we find an intrinsic linewidth of FWHM 140 to 150 km/s to reproduce the measured velocity-position diagrams (see also Paper I).

These numbers show that a gas disk consisting of a system of differentially precessing rings observed in a finite beam can account for most of the observed line width. The remaining contribution to the line width of FWHM 50 to 70 km/s corresponds to a velocity dispersion of 20 to 30 km/s and is within the errors in agreement with the velocity dispersion of 6-10 km/s derived for giant molecular cloud complexes in our Galaxy. Such a comparison, however, is not straightforward to make, since there is no spiral galaxy like disk in Cen A and the molecular material is always well within the bulge of the elliptical galaxy.

Additional indications that the velocity dispersion of molecular cloud complexes is close to the galactic value comes from the different absorption features (Paper II) that spread over a range of 40 km/s with line widths of 4 to about 10 km/s and from the sharpness of the triangular emission line profiles observed off the nuclear position towards Centaurus A (see also Quillen et al. 1992).

We also compared the integrated emission line intensity distribution predicted by the model of Quillen et al. (1992) with the measured distributions in the ^{12}CO(1–0) and ^{12}CO(2–1) line. We compared their model with our maps by calculating ratios of one dimensional cuts in maps with 45″ resolution at a position angle of 125^o through the emission peaks at $\pm$50″ from the center along the gas disk. These ratios, displayed in Fig. 7, are flat within the estimated errors of 10% to 15% and demonstrate qualitatively the similarity of the observed maps with the predicted map. This shows for the first time that the model also agrees with a complete, fully sampled map in the ^{12}CO(2–1) emission line and not only applies to the ^{12}CO(1–0) map of Paper I as already mentioned by Quillen et al. (1992).

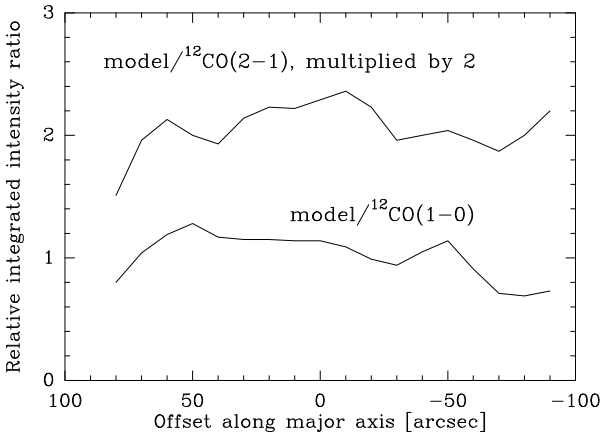

Fig. 7. Comparison of the measured integrated intensity along the dust lane with the prediction from the kinematic model of Quillen et al. (1992). See the text for details. The curve for ^{12}CO (2–1) has been multiplied by 2. Estimated errors of the ratio are 10% to 15%.

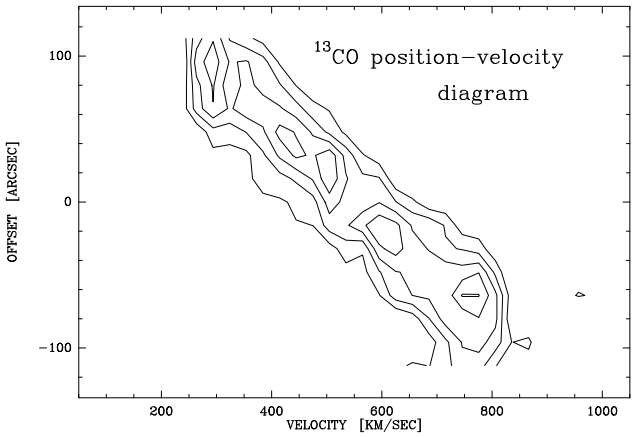

Fig. 8. Position-velocity diagram of the ^{13}CO 1–0 emission along the dust lane of Centaurus A (position angle 125°). The inner 130″ show the signature of solid body rotation.

It is instructive to compare the position-velocity information of the optically thick ^{12}CO lines with more optically thin tracers like ^{13}CO which allow us to sample more deeply into the molecular gas. Fig. 8 shows the position-velocity diagram of the ^{13}CO 1–0 data along the dust lane (position angle 125°). The diagram is indicative for a solid body rotation in the inner 130″ and thus similar to the result obtained from the ^{12}CO 1–0 data (Paper I). The transition between the rising and flat part of the rotation curve at velocities of about 300 and 800 km s^{-1} seen in the ^{12}CO data appears as well in our ^{13}CO position-velocity diagram. However, the transition is not as clearly visible due to the smaller spatial coverage of the ^{13}CO observations.

4. Summary and concluding remarks

The main results of our investigation can be summarized as follows:

1. The ^{13}CO J=1–0 map of Centaurus A is morphologically similar to the ^{12}CO 1–0 and 2–1 maps. The position-velocity diagram of the ^{13}CO emission indicates solid body rotation for the inner 130″ (2 kpc).
2. The molecular emission line ratios of ^{12}CO, ^{13}CO and C^{18}O are indicative of warm, dense, optically thick gas. Maps of the ^{12}CO 2–1/1–0 and ^{12}CO/^{13}CO 1–0 ratios across the dust lane show values which lie within the range as found in other galaxies. Apart from a higher ^{12}CO 2–1/1–0 ratio in the southeastern part of the dust lane, no large variation of the line ratios is found across the disk at a spatial resolution of 44″.
3. Simple one component radiative transfer calculations indicate a kinetic temperature of 10–15 K, H_2 number density of $1 - 3 \times 10^4$ cm^{-3}, and beam averaged CO column density of $3 - 4 \times 10^{17}$ cm^{-2} for the center and a northwestern position in the disk. The molecular gas is warmer ($T_{\rm kin}$ = 20–30 K) in the southeastern part of the disk, and the CO column density is higher (1×10^{18} cm^{-2}). The differences between the SE and NW part of the dust lane may be due to a greater star-formation activity in the SE. The deduced H_2 mass for Centaurus A is 1.2×10^8 M$_\odot$.
4. The upper limit of the C^{18}O opacity of the absorbing molecular gas, $\tau_{18} < 0.02$, (derived from the non-detection of the C^{18}O absorption at the systemic velocity of Cen A) indicates a deficiency of C^{18}O in the diffuse molecular gas responsible for the central absorption feature.
5. The observed ^{12}CO J=2–1 intensity is consistent with the molecular gas being distributed in a thin, warped disk consisting of differentially precessing rings as modelled by Quillen et al. (1992). Comparison of the observed ^{12}CO J=2–1 intensity with the model predictions shows good agreement.

In general it is quite difficult to find CO emission from ellipticals, although some detections have been reported (e.g. Lees et al. 1991, Sage and Galleta 1993, Wiklind et al. 1995, Knapp and Rupen 1996). It appears that elliptical galaxies like Centaurus A cannot be very common.

The investigations of the molecular gas in Centaurus A that have been carried out over the recent years have shown that abundances, excitation temperature, and density of the emitting molecular gas (this paper, Paper I, Phillips et al. 1987, Israel et al. 1990) in the disk of Centaurus A are similar to the values obtained for the disk material in other galaxies. The comparison shows that the ISM of Centaurus A has global properties which are intermediate between those found for the bulges of the Galaxy and spiral galaxies with a starburst nucleus like IC342.

Acknowledgements. We want to thank the SEST staff for their support during the observations, and R. Genzel for making accessible an unpublished [CII] map. WW wants to thank the MPI für extraterrestrische Physik for the hospitality while working on this paper.

References

Bland, J., Taylor, K., and Atherton, P.D. 1987, *M.N.R.A.S.* 228, 595.

Crawford, M.K., Genzel, R., Townes, C.H., and Watson, D.M. 1985, *Ap.J.* 291, 755.
de Vaucouleurs, G. 1979, *Astron.J.* 84, 1270.
Dufour et al. 1979, *Astron.J.* 84, 284.
Paper I: Eckart A., Cameron, M., Rothermel, H., Wild, W., Zinnecker, H., Rydbeck, G., Olberg, M., and Wiklind, T. 1990a, *Ap.J.* 363, 451.
Paper II: Eckart A., Cameron, M., Genzel, R., Jackson, J.M., Rothermel, H., Stutzki, J., Rydbeck, G., and Wiklind, T. 1990b, *Ap.J.* 365, 522.
Eckart, A., Downes, D., Genzel, R., Harris, A.I., Jaffe, D.T. and Wild, W. 1990c, *Ap.J.* 348, 434.
Graham, J.A. 1979, *Ap.J.* 232, 60.
Graedel, T.E., Langer, W.D., and Frerking, M.A. 1982, *Ap.J.(Suppl.)* 48, 321.
Israel, F.P., van Dishoek, E.F., Baas, F., Kornneef, J., Black, J.H., and de Graauw, T., 1990, *Astr. Ap.* 227, 342.
Israel, F.P., van Dishoek, E.F., Baas, F., de Graauw, T., and Phillis, T.G. 1991, *Astr. Ap.* 245, L13.
Joy, M., Lester, D.F., Harvey, P.M., and Ellis, H.B. 1988, *Ap.J.* 326, 662.
Knapp, G.R., and Rupen, M.P. 1996, *Ap.J.* 460, 271.
Lees, J.F., Knapp, G.R., Rupen, M.P., and Phillips, T.G. 1991, *Ap.J.* 379, 177.
Madden, S.C., Genzel, R., Herrmann, F., Poglitsch, A., Geis, N., Townes, C.H., and Stacey, G.J. 1992, *BAAS* 181, 9305.
Marston, A.P., and Dickens, R.J. 1988, *Astr. Ap.* 193, 27.
Martin, H.M., Sanders, D.B., and Hills, R.E. 1984, *M.N.R.A.S.* 208, 35.
Millar, T.J., and Freeman, A. 1984, *M.N.R.A.S.* 207, 425.
Nicholson, R.A., Bland-Hawthorn, J., and Taylor, K. 1992, *Ap.J.* 387, 503.
Phillips, T.G., Ellison, B.N., Keene, J.B., Leighton, R.B., Howard, R.J., Masson, C.R., Sanders, D.B., Veidt, B., and Young, K. 1987, *Ap.J.(Letters)* 322, L73.
Preston, R.A., Wehrle, A.E., Morabito, D.D., Jauncey, D.L., Batty, R.F., Haynes, R.F., Wrigth, A.E.,and Nicolson, G.D. 1983, *Ap.J.* 266, L93.
Quillen, A.C., de Zeeuw, P.T., Phinney, E.S., and Phillips, T.G. 1992, *Ap.J.* 391, 121.
Paper III: Rydbeck G., Wiklind, T., Cameron, M., Wild, W., Eckart, A., Genzel, R., and Rothermel, H., 1993, *Astr. Ap. (Letters)* 270, L13.
Sage, L.J., and Galleta, G. 1993, *Ap.J.* 419, 544.
Sage, L.J., and Isbell, D.W. 1991, *Astr. Ap.* 247, 320.
Seaquist, E.R., and Bell, M.B. 1990, *Ap.J.* 364, 94.
van Gorkom, J.H. 1987, in *IAU Symposium 127, Structure and Dynamics of Elliptical Galaxies,* ed. T. de Zeeuw (Dordrecht:Reidel), p.421.
van Gorkom, J.H., van der Hulst, J.M., Haschick, A.D. , and Tubbs, A.D. 1990, *Astron.J.* 99, 1781.
Wannier, P.G. 1980, *Ann. Rev. Astron. Astrophys.* 18, 399.
Wiklind, T., Combes, F., and Henkel, C. 1995, *Astr. Ap.* 297, 643.
Wilson, T.L.,and Matteuchi, F. 1992, *Astr. Ap. Rev.* 4, 1.
Young, J.S., and Sanders, D.B. 1986, *Ap.J.* 302, 680.

This article was processed by the author using Springer-Verlag LaTeX A&A style file *L-AA* version 3.